Pergamon

PII: S0191–8141(98)00006–6

Journal of Structural Geology, Vol. 20, No. 6, pp. 673 to 680, 1998

0191-8141/98 $19.00 + 0.00

Melt-bearing shear zones: analogue experiments and comparison with examples from southern Madagascar

DJORDJE GRUJIC

Geologisches Institut, Albert-Ludwigs-Universität Freiburg, D-79104 Freiburg, Germany
E-mail: grujic@perm.geologie.uni-freiburg.de

and

NEIL S. MANCKTELOW

Geologisches Institut, ETH-Zentrum, CH-8092 Zürich, Switzerland

(*Received* 14 *April* 1997; *accepted in revised form* 13 *January* 1998)

Abstract—Analogue model experiments were conducted to investigate the influence of irregularly distributed weak sites in localising strain, as an aid to understanding shear zone development in partially molten rocks. The very weak inclusions consisted of Vaseline in a homogeneous matrix of paraffin wax, which has a power-law viscous rheology. Boundary conditions were those of pure shear at constant natural strain rate and confining stress σ_3. The inclusions were initially perfect cylinders with axes parallel to the intermediate bulk strain axis Y. Conjugate shear zones nucleate on the inclusions and link up to form an anastomosing pattern of high strain zones of concentrated shear surrounding much more weakly deformed pods of near coaxial strain. The zones initiate at angles near 45° to the bulk shortening axis Z but stretch and rotate towards the X axis with increasing bulk strain. All inclusions nucleate shear zones, so that with increasing development of the anastomosing pattern, weak material occurs only within the high strain zones. The restriction of migmatite leucosomes to shear zones in natural examples could also reflect a corresponding control of melt on the sites of shear zone nucleation, rather than implying accumulation from the surrounding wall-rock. The model geometry is very similar to that observed in small-scale shear zones in migmatites of southern Madagascar. Elongate zones rich in weak inclusions, originally either perpendicular or at 45° to the Z axis, were also modelled for direct comparison with the regional-scale geometry of the Pan-African high-grade 'shear zones' on Madagascar.

INTRODUCTION

Shear zones are recognised in the field on all scales as elongate, approximately planar zones of high strain (Ramsay, 1980). Tight observational constraints on the strain geometry are rarely available, although it is often assumed that they correspond to simple shear. If the adjacent walls are rigid, then the length of the shear zone must remain constant during deformation and the only possible solutions involve some combination of perfect simple shear parallel to the walls and width change perpendicular to the walls, due to variation in volume (e.g. Ramsay and Graham, 1970). This restriction is removed if the walls are deformable (e.g. Means, 1989), as is certainly the case in lower crustal shear zones developed at high metamorphic grade. Such high-grade shear zones are commonly intimately associated with partial melting and migmatite development, with leucosome material concentrated in the zones themselves (e.g. Brown *et al.*, 1995). This study presents the results of analogue-model experiments considering the geometry of high-grade shear zones, both on the outcrop scale, where melt is generally distributed in an irregular anticlustered pattern, and on the larger map-scale, where syntectonic intrusions are often restricted to major regional shear zones. The strain pattern developed in these analogue models, which were deformed with boundary conditions of pure shear, is very similar to the natural examples and demonstrates that the automatic assumption of near simple shear kinematics (e.g. major strike-slip displacement for steep shear zones) can lead to incorrect interpretations of the regional tectonics.

EXPERIMENTAL METHODS

The effect of partial melt on the initiation and development of shear zones was modelled as a distribution of very weak inclusions in a homogeneous ductile matrix. The volume of this weak phase remains constant during the experiments and thus only the mechanical effect of 'melt' on the strain distribution is investigated. The probable feedback effect, where concentrated deformation and/or spatial variation in mean stress (≈'pressure') promote localised additional partial melting, is not considered. The influence of isolated weak inclusions on the strain distribution in the surrounding matrix has already been studied both by analogue (Baumann, 1986; Baumann and Mancktelow, 1987) and by numerical modelling (Genter, 1993). These studies have shown that, as might be expected, the weaker inclusions take up a larger proportion of the bulk strain, and that this strain concentration is

accommodated in the surrounding matrix by zones of concentrated shear deformation. The width of this perturbed zone is a function of the size and shape of the inclusion and probably also of the viscosity ratio.

The analogue model experiments for this study were performed under pure-shear, plane-strain boundary conditions using an upgraded version of the deformation rig described by Mancktelow (1988a). Models were made of paraffin wax with melting range 46–48°C (Mancktelow, 1988b) and the weak inclusions consist of Vaseline. The viscosity ratio for the experimental conditions (24 ± 0.1°C, strain rate $3 \times 10^{-5}\,s^{-1}$) is ~300:1. Narrow layers of weaker paraffin wax of melting range 40–42°C were placed between the confining side plates and the model block to diminish the effect of the straight side boundary constraint, which otherwise tends to dampen the propagation of zones of heterogeneous deformation toward the boundary.

In all cases, the initial form of individual weak inclusions was cylindrical, with a circular cross-section in the *XZ* plane and the cylinder axis parallel to the intermediate bulk strain axis *Y* (Fig. 1). Two series of experiments were performed, one with an unclustered distribution of inclusions to simulate the outcrop-scale distribution of melt and one with planar zones of clustered inclusions to simulate the heterogeneous distribution often observed on a regional scale. In the following we present the experimental results and their comparison with natural examples of strain localisation in very weak sites.

EXPERIMENTAL RESULTS AND DISCUSSION

Unclustered distribution of inclusions

A typical example with 8 volume% weak inclusions is shown in Fig. 2, which illustrates the important geometrical characteristics of this series of experiments.

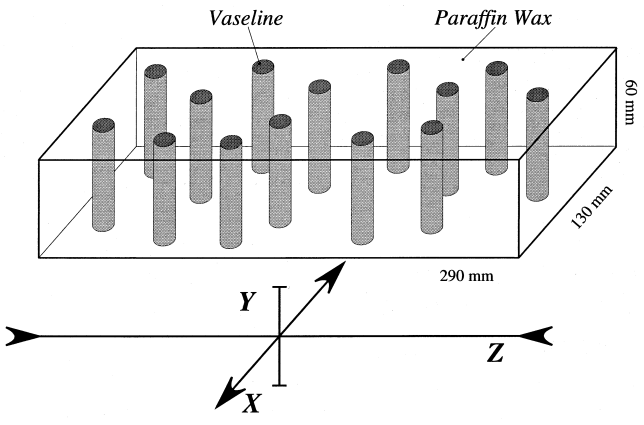

Fig. 1. Model geometry, showing the orientation with respect to the *XYZ* axes of bulk strain for the imposed pure-shear deformation and the initial form of Vaseline inclusions. The cross-section of the cylindrical inclusions in the *XZ* plane is circular and the cylinder axes are parallel to the intermediate axis *Y*.

The initially cylindrical weak inclusions are flattened in the overall bulk *XY* plane, with short, conjugate shear zones initiating at the tips of the now elongate inclusions. The strain in the weak sites—indicated by the axial ratio of elongate inclusions—is much higher than the strain in the neighbouring matrix but it is also larger than the bulk strain. With increasing bulk strain, the shear zones progressively propagate into the adjacent matrix and arrays of weak inclusions of suitable orientation are interconnected to form larger shear zones. These shear zones are also conjugate and, in the course of deformation, rotate toward the flattening plane to produce increasingly acute angles between conjugate shear zones containing the bulk extension direction *X*. The conjugate shear zones enclose less deformed (to almost undeformed) lens-shaped pods of matrix, within which deformation closely approximates coaxial pure shear. This geometry is very similar to the model proposed by Bell (1981) for the heterogeneous deformation during progressive pure shear. It also mimics the natural anastomosing shear zones described in granitic plutons strained under mid- to high-grade metamorphic conditions (e.g. Simpson, 1982; Gapais *et al.*, 1987), and the internal geometry of some mylonite zones (e.g. Bell and Hammond, 1984). Most natural ductile shear zones which are conjugate show an obtuse angle facing the maximum regional shortening direction. It has always been a problem to decide if this relationship is original or if—as we suggest—it is the result of a deformation of the rock lozenges between the shear zones (see Ramsay and Huber, 1987, fig. 26.29).

The progressive development of the shear zones is better seen in models with a lower density of weak inclusions (Fig. 2b). At higher concentration, the interconnection of shear zones is more rapidly established due to the closer spacing of weak inclusions. The heterogeneity of deformation is also a function of scale. At the same scale of observation and for the same volume proportions of strong and weak material, it is clear that deformation will appear more homogeneous for a large number of very small weak inclusions than for a smaller number of large inclusions.

Since the interconnected shear zones always nucleate on the weak inclusions, all the weak phase (representing melt) comes to lie within high-strain shear zones, even for fairly low bulk strains (e.g. Fig. 2b). The restriction of migmatite leucosomes to shear zones in natural examples could also reflect a corresponding dominant control on the sites of shear zone nucleation, rather than exclusively implying accumulation from the surrounding wall-rock.

Clustered distribution of very weak inclusions

In these experiments the weak inclusions are restricted to relatively narrow planar zones perpendicular (Fig. 3a) or oblique (Fig. 3b) to the bulk shortening

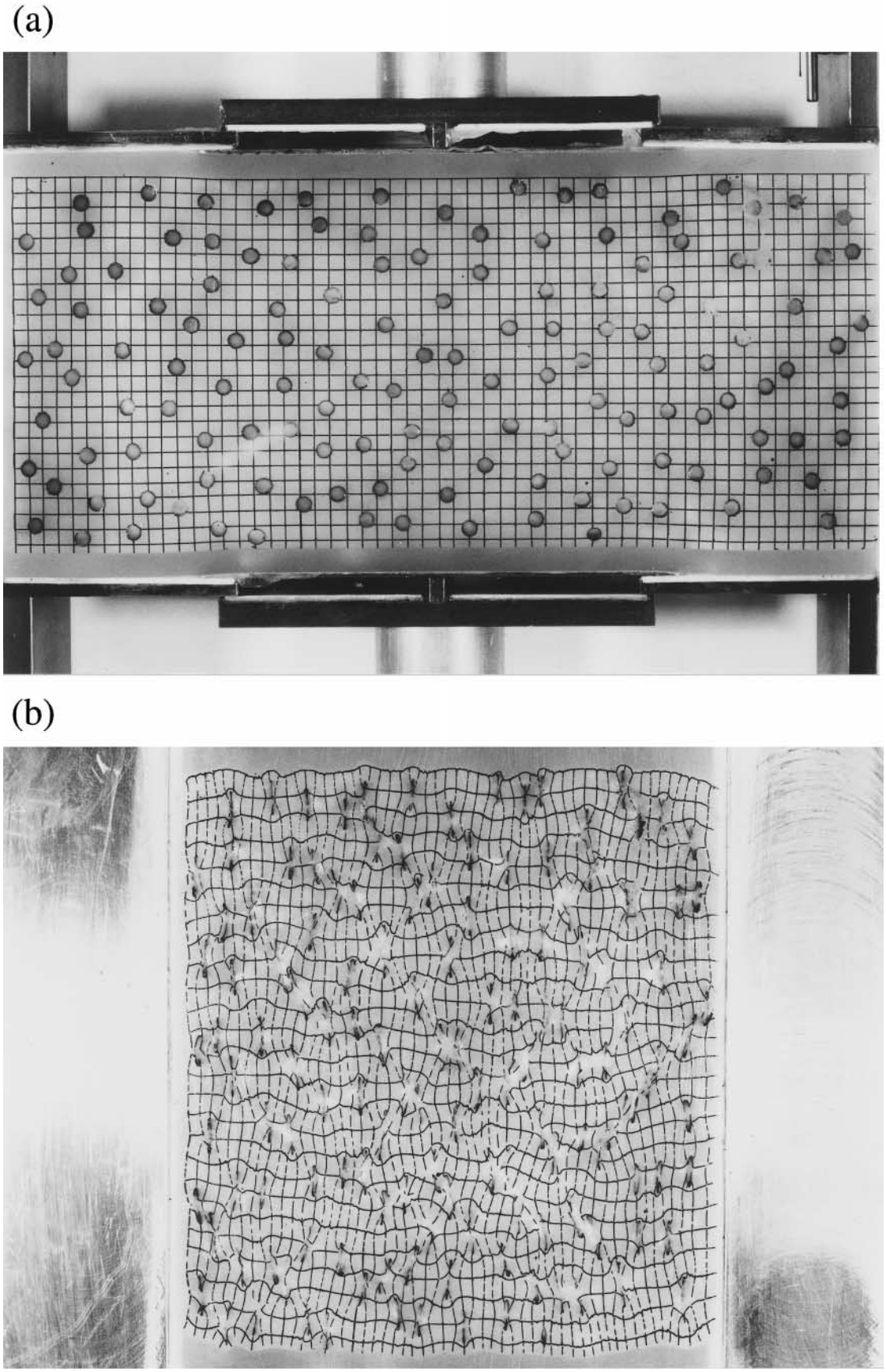

Fig. 2. Photographs of a model with 8 volume% of randomly distributed weak inclusions taken at (a) 0%, and (b) 40% shortening, viewed in the *XZ* plane. The initial undeformed spacing between the grid lines in the model was 5 mm.

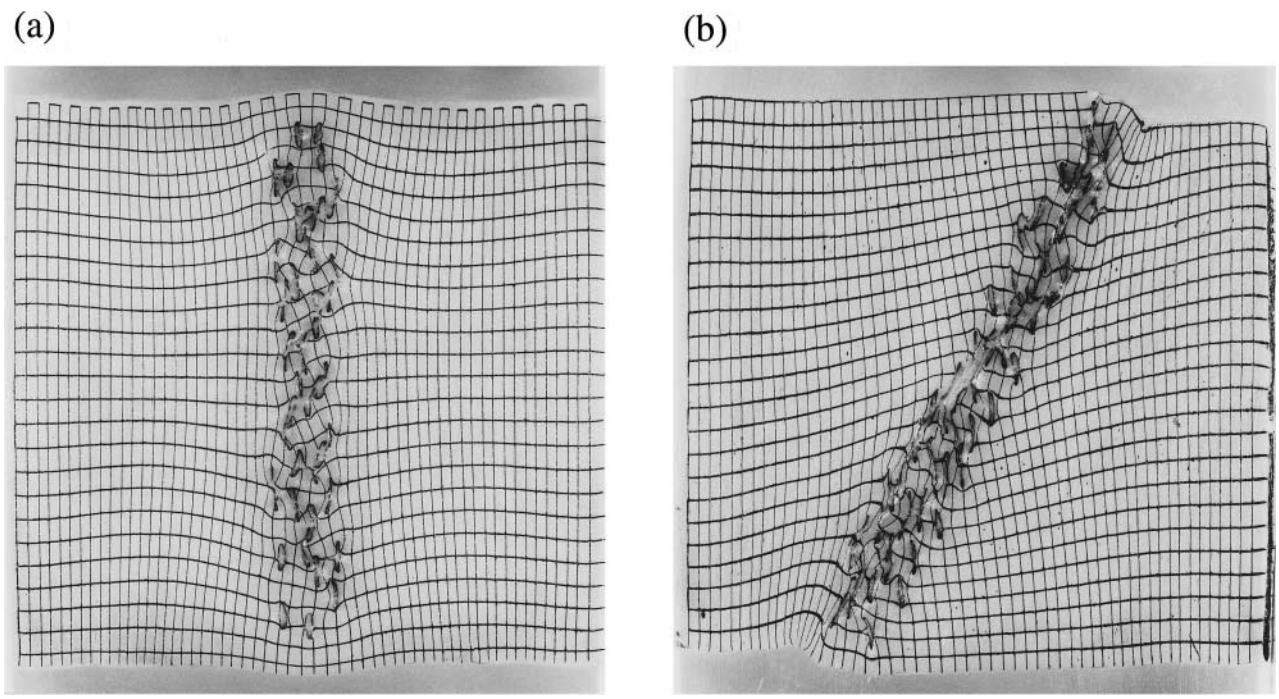

Fig. 3. Photographs of models with weak inclusions distributed in a zone (a) perpendicular, and (b) initially at 45° to the shortening direction, taken at 40% shortening, viewed in the *XZ* plane. After deformation the weak zone is at 63° to the shortening direction (rotation of 18°) and shows an extension of $e = 0.23$. The initial undeformed spacing between the grid lines in the models was 5 mm.

direction. The behaviour of the two-phase material within these zones is analogous to that described above, with anastomosing shear zones surrounding pods of material exhibiting weaker, nearly coaxial deformation. On a broader scale, there is a clear concentration of strain within the zone of weak inclusions and, again as described above, increasing deformation causes the shear zones to progressively rotate and extend, such that the angle between the conjugate sets decreases. Thus, at higher bulk strain, the two-phase zone appears as a high strain planar zone consisting of anastomosing but on average near-parallel shear zones with *alternating* senses of shear. In nature, this would appear as a strongly foliated zone within a much more weakly foliated regional block, and would be mapped as a shear zone. However, there could be some difficulty in obtaining a consistent shear sense from kinematic indicators. As can be seen from Fig. 3, if the zone was initially at a high angle to the regional shortening direction, then there is no significant displacement across the 'shear zone'. In contrast, if the planar zone is oblique to the bulk strain it will initiate a major shear zone whose kinematics will depend on the initial zone orientation with respect to the regional shortening direction. Both the smaller-scale shear zones developed in the weaker zone and the zone itself are progressively elongated parallel to their length and correspond to *stretching faults* as described by Means (1989).

COMPARISON WITH NATURAL EXAMPLES

A natural example on regional and outcrop scale of a strain distribution similar to that observed in the analogue experiments, with a clustered distribution of weak inclusions, can be found in the basement of southern Madagascar. Precambrian basement, of at least early Proterozoic age (Paquette *et al.*, 1994), has been strongly deformed under high-temperature low-pressure conditions, and intruded by numerous granitic intrusions during the Pan-African orogenesis between 560 and 510 Ma (Nicollet, 1990; Paquette *et al.*, 1994). On the regional scale, deformation produced three major shear zones (Fig. 4) with sub-vertical mylonitic foliation, and a sub-horizontal stretching lineation (Martelat *et al.*, 1997). Two shear zones are oriented approximately N–S (Ampanihy and Beraketa shear zones). The third one is sinistral and oriented NW–SE (the Bongolava–Ranotsara shear zone). The N–S shear zones, 10–20 km in width, extend for at least 300 km. These two shear zones were only recently recognised and have been the subject of various kinematic interpretations. In the first known description, the Ampanihy shear zone was defined as dextral (Rolin, 1991), in the second as sinistral (Martelat *et al.*, 1997), and in the third interpretation as a zone of intensive flattening, initially representing a thrust (De Wit *et al.*, 1993). From our field observations and in the light of the current study, we consider that these N–S oriented

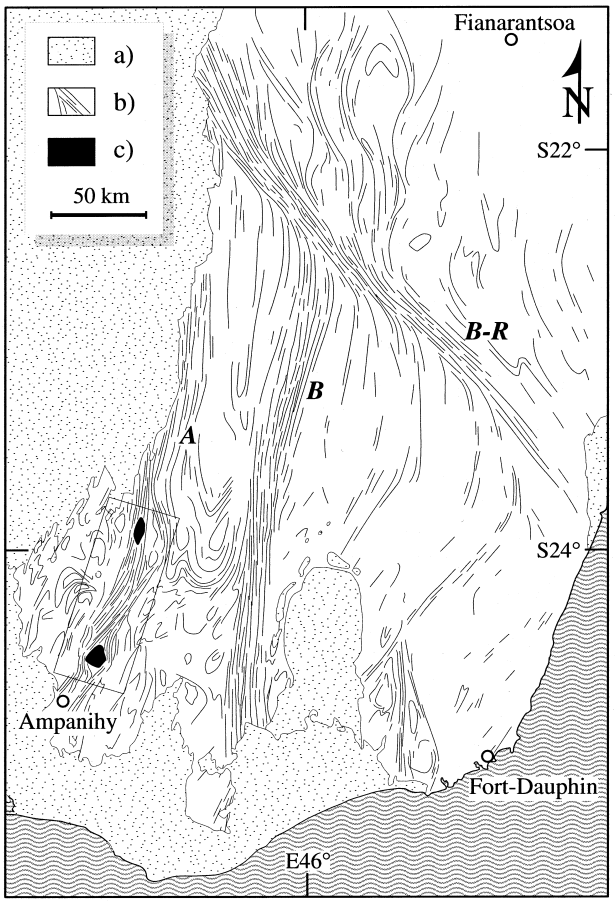

Fig. 4. Simplified structural map of the basement in southern Madagascar showing the trend of major shear zones: A: Ampanihy, B: Beraketa, B–R: Bongolava–Ranotsara shear zone; (a) Phanerozoic sediments and volcanics; (b) Precambrian basement and Pan-African intrusives with trend of foliation indicated; (c) anorthosite. The box in the south-west corner marks the part of the Ampanihy shear zone containing two anorthosite bodies. This situation was simulated in the experiment presented in Fig. 6. Geological boundaries after Besairie (1964), and the regional foliation trajectories after Martelat *et al.* (1997).

zones were initiated in areas of more common syntectonic granitic intrusions and underwent strong flattening normal to their strike and stretching parallel to it, but with no dominant sense of vorticity. The bulk-strain geometry can be demonstrated by an analysis of the distribution of leucosomes in outcrop-scale shear zones. Sub-circular pods of leucosome fill the necks of sub-vertical internal boudins (Fig. 5a). Conjugate shear zones containing leucosome are common, with the acute angle between them containing the strike direction of the master shear zone (Fig. 5b). The latest folds have sub-vertical axes, and their axial planes usually contain leucosome (Fig. 5c). The folds are strongly asymmetric, but have both S and Z shapes within the same structural domain and, therefore, cannot be used as kinematic indicators. Leucosomes oriented sub-parallel to the mylonitic foliation are symmetrically boudinaged with the boudin-axes sub-vertical (Fig. 5d). Moreover, the Ampanihy shear zone also contains two anorthosite massifs (Boulanger, 1959; Ashwal *et al.*, 1995). They are much older than the shear zones and behaved as effectively rigid inclusions during shearing (Fig. 4). The southern anorthosite massif is asymmetric in map view with pressure shadow-like tails. Its shape suggests dextral major shear (sinistral by Martelat *et al.*, 1997, fig. 12). As it has been shown in previous analogue experiments (Ildefonse *et al.*, 1992; Ildefonse and Mancktelow, 1993), the sense of rotation of an elongate rigid inclusion (for both pure and simple shear boundary conditions) depends on its initial orientation and shape, and 'anomalous' shear sense indicators can often be found. This is emphasised if slip or shear is concentrated at the interface between inclusion and matrix. The presence of the anorthosite bodies was simulated in our experiments by two rigid inclusions within the zone of weak inclusions (Fig. 6a). In the *XZ* plane one rigid inclusion was round, and the other was elongated with an axial ratio of 3:1 and initially oriented at 45° to the shortening direction. As expected, the cylindrical inclusion did not rotate, while the elongated one underwent a dextral rotation consistent with its initial obliquity (Fig. 6b). Midway between the two rigid inclusions, the weak zone as a whole shows necking due to differential shortening caused by the rigid inclusions. Within the boudin neck there is a dominant dextral shear zone and a weaker, conjugate sinistral shear zone. This situation is very similar to the Ampanihy shear zone: the zone is thinnest in the area between the two anorthosite massifs and in that area it shows a slight dextral offset (Martelat *et al.*, 1997, fig. 3).

A similar situation might be responsible for the ambiguities surrounding the crustal-scale, granulite-facies shear zones of the Nagssugtoqidian orogen, SW Greenland. Here again, the sense of shear is a subject of various interpretations, and the shear zones are associated with synkinematic dikes (Hanmer *et al.*, 1997, and references therein). Some of the major crustal shear zones (that have been taken as type examples of high-grade shear zones) are now shown to be an array of high strain zones with no significant lateral displacement (e.g. Hanmer *et al.*, 1997). Bell (1981) also concluded that mylonite zones could also form by progressive, bulk, inhomogeneous shortening. The important factor is the scale of observation. Overall, the deformation in all our analogue models was pure shear, but at a smaller scale individual anastomosing shear zones were developed. These were not 'simple shear zones' however, but are stretched and rotated during their development, with the simple shear component in general decreasing during the deformation history.

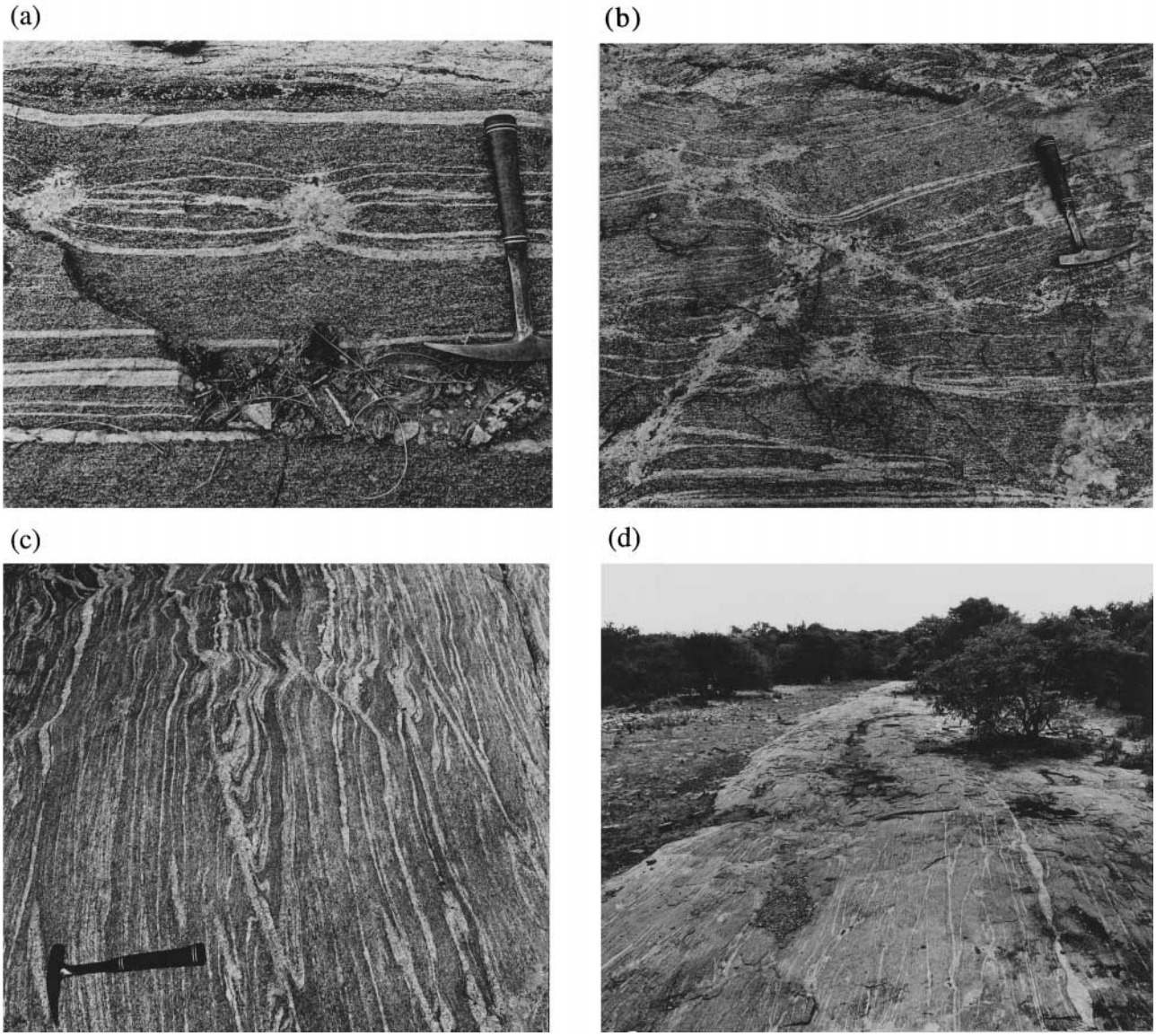

Fig. 5. Photographs of migmatites in the Ampanihy shear zone near the village of Ampanihy, southern Madagascar. The main foliation is sub-vertical and strikes approximately NNE–SSW, the stretching lineation is sub-horizontal. (a) Sub-circular pods of leucosome filling the necks of sub-vertical internal boudins; (b) dextral and sinistral shear zones localised on the leucosome sites; (c) the latest folds with sub-vertical axes, and axial planes usually containing leucosome; (d) planar leucosomes oriented sub-parallel to the mylonitic foliation that are boudinaged with the longer boudin-axes sub-vertical. Photographs (a) and (b) are viewed looking down, with top to the west; photographs (c) and (d) are viewed toward the north. Scale is provided by the geological hammer.

CONCLUSIONS

The presence of very weak inclusions, such as the patches of melt typical of high-grade rocks in the lower crust, results in a very characteristic strain pattern during deformation. Conjugate shear zones nucleate on the inclusions and link up to form an anastomosing pattern of high strain zones of concentrated shear surrounding much more weakly deformed pods of near coaxial strain. The high strain zones are not 'simple shear zones', since they are stretched and rotated during bulk deformation. Due to this rotation, the angle between zones of opposite shear sense decreases with increased bulk deformation. Rotating shear zones and their deformable walls might allow conjugate sets to operate simultaneously. Moreover, the synkinematic elongation lineation in the wall-rocks is not necessarily parallel to the shear direction as it is a finite strain feature. Recent high-precision dating has provided evidence that the melt can be present in the deep crust for a period of time long enough to accommodate significant amounts of deformation (Berger *et al.*, 1997). Zones with a higher degree of partial melting (or more thoroughly intruded by melt) will concentrate strain and develop such an anastomosing foliation pattern, which at high strain will be semi-parallel. On the regional scale, such zones would be mapped as shear zones, but the internal shear sense from kinematic indicators will be frustratingly inconsistent, crystallographic preferred orientation patterns

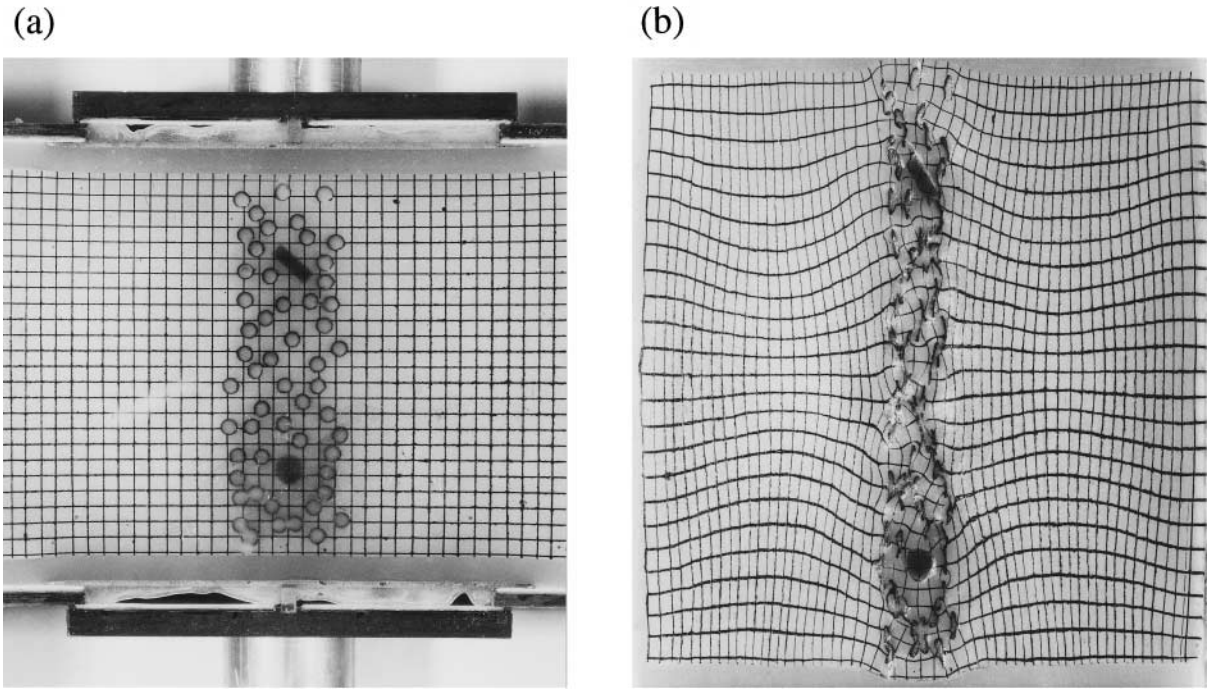

Fig. 6. Photographs of a planar zone of weak inclusions, initially perpendicular to the shortening direction. Two rigid inclusions were placed in the middle of the weak zone. The lower one was circular in cross section, the upper one was rectangular, with initial axial ration 3:1 and initial orientation of 45° to the shortening direction. (b) Same as (a) after 40% shortening. The initial undeformed spacing between the grid lines in the models was 5 mm.

will also be inconclusive and may often be close to symmetrical (e.g. crossed-girdle *c*-axis patterns in quartz), and the actual shear offset across the 'shear zone' may be small compared to the strength of internal fabric development.

Acknowledgements—We thank A. Berger, Y. Podlachnikov, J. G. Ramsay, C. L. Rosenberg and D. C. Tanner for stimulating discussions on the relation between melt and deformation. The manuscript benefitted from reviews by T. Bell, R. J. Norris, and C. J. L. Wilson. Financial support from the ETH Research Credit 2-77-652-92 and the Schweizerische Nationalfond Project 0-20-154-86 is gratefully acknowledged. D. G. also acknowledges financial support from the ENS Lyon for the field work in Madagascar in 1993. Inestimable help to D. G. was provided by D. Pejcinovic in arranging support in the field and in the laboratory.

REFERENCES

Ashwal, L. D., Morel, V. P. I. and Hamilton, M. A. (1995) Rb–Sr and Sm–Nd geochronology of the massif-type anorthosites, Southwest Madagascar. *Centennial Geocongress, Geological Society of South Africa* **1,** 206–209.

Baumann, M. T. (1986) Verformungverstelung an Scherzonenenden: Analogmodelle und natürliche Beispile. Unpublished Ph.D. thesis, ETH Zürich, Switzerland.

Baumann, M. T. and Mancktelow, N. S. (1987) Initiation and propagation of ductile shear zones. *Terra Cognita* **7,** 47.

Bell, T. H. (1981) Foliation development—the contribution, geometry and significance of progressive, bulk, inhomogeneous shortening. *Tectonophysics* **75,** 273–296.

Bell, T. H. and Hammond, R. L. (1984) On the internal geometry of mylonite zones. *Journal of Geology* **92,** 667–686.

Berger, A., Rosenberg, C., Oberli, F., Meier, M. and Gieré, R. (1997) For how long can melt be present in a pluton? Constraints from isotope dating. *Abstracts Supplement 1, Terra Nova* **9,** 458.

Besairie, H. (1964) *Madagascar: Carte géologique 1:1,000,000*. Service géologique de Madagascar, Antananarivo.

Boulanger, J. (1959) Les anorthosites de Madagascar. *Annales Géologiques de Madagascar* **26,** 71.

Brown, M., Averkin, Y. A. and McLellan, E. L. (1995) Melt segregation in migmatites. *Journal of Geophysical Research* **100**(B8), 15,655–15,679.

De Wit, M. J., Ashwal, L., Bowring, S. A., Isachsen, C. E. and Rambeloson, R. (1993) Pan-Gondwanian structures: Tectonic studies in southern Madagascar. *Geological Society of America, Abstracts with Programs* **25,** 232.

Gapais, D., Bale, P., Choukroune, P., Cobbold, P. R., Mahjoub, Y. and Marquer, D. (1987) Bulk kinematics from shear zone patterns: some field examples. *Journal of Structural Geology* **9,** 635–646.

Genter, M. A. (1993) Analytical and numerical considerations on the initiation and propagation of ductile shear zones in elastic-thermoviscous power law materials. Unpublished Ph.D. thesis, ETH Zürich, Switzerland.

Hanmer, S., Mengel, F., Connelly, J. and Van Gool, J. (1997) Significance of crustal-scale shear zones and synkinematic mafic dykes in the Nagssugtoqidian orogen, SW Greenland: a re-examination. *Journal of Structural Geology* **19,** 59–75.

Ildefonse, B. and Mancktelow, N. S. (1993) Deformation around rigid particles: the influence of slip at the particle/matrix interface. *Tectonophysics* **221,** 345–359.

Ildefonse, B., Sokoutis, D. and Mancktelow, N. S. (1992) Mechanical interactions between rigid particles in a deforming ductile matrix. Analogue experiments in simple shear flow. *Journal of Structural Geology* **14,** 1253–1266.

Mancktelow, N. S. (1988a) An automated machine for pure shear deformation of analogue materials in plane strain. *Journal of Structural Geology* **10,** 101–108.

Mancktelow, N. S. (1988b) The rheology of paraffin wax and its usefulness as an analogue for rocks. In *Geological Kinematics and Dynamics (in Honour of the 70th Birthday of Hans Ramberg)*. Bulletin of the Geological Institution, University of Uppsala. **14,** 181–193.

Martelat, J.-E., Nicollet, C., Lardeaux, J.-M., Vidal, G. and Rakotondrazafy, R. (1997) Lithospheric tectonic structures developed under high-grade metamorphism in the southern part of Madagascar. *Geodynamica Acta* **10,** 94–114.

Means, W. D. (1989) Stretching faults. *Geology* **17,** 893–896.

Nicollet, C. (1990) Crustal evolution of the granulites of Madagascar. In *Granulites and Crustal Evolution*, ed. D. Vielzeuf and Ph. Vidal, Vol. 311, pp. 210–291. Kluwer Academic Publishers.

Paquette, J-L., Nédélec, A., Moine, B. and Rakotondrazafy, M. (1994) U–Pb, single zircon Pb-evaporation, and Sm–Nd isotopic study of a granulite domain in SE Madagascar. *Journal of Geology* **102,** 523–538.

Ramsay, J. G. (1980) Shear zone geometry: a review. *Journal of Structural Geology* **2,** 83–99.

Ramsay, J. G. and Graham, R. H. (1970) Strain variation in shear belts. *Canadian Journal of Earth Sciences* **7,** 786–813.

Ramsay, J. G. and Huber, M. I. (1987) *The Techniques of Modern Structural Geology. Volume 2: Folds and Fractures*. Academic Press, London.

Rolin, P. (1991) Présence de décrochements précambriens dans le bouclier méridional de Madagascar: implications structurales et géodinamiques. *Comptes Rendus de l'Académie des Sciences, Paris* **312,** 625–629.

Simpson, C. (1982) The structure of the northern lobe of the Maggia Nappe, Ticino, Switzerland. *Ecologae Geologicae Helvetiae* **75,** 495–516.